K. W. Stafford, L. Rosales-Lagarde, and P. J. Boston – Castile evaporite karst potential map of the Gypsum Plain, Eddy County, New Mexico and Culberson County, Texas: A GIS methodological comparison. *Journal of Cave and Karst Studies,* v. 70, no. 1, p. 35–46.

CASTILE EVAPORITE KARST POTENTIAL MAP OF THE GYPSUM PLAIN, EDDY COUNTY, NEW MEXICO AND CULBERSON COUNTY, TEXAS: A GIS METHODOLOGICAL COMPARISON

KEVIN W. STAFFORD[1,2], LAURA ROSALES-LAGARDE[1,2], AND PENELOPE J. BOSTON[1,2]

Abstract: Castile Formation gypsum crops out over ~1,800 km^2 in the western Delaware Basin where it forms the majority of the Gypsum Plain. Karst development is well recognized in the Gypsum Plain (i.e., filled and open sinkholes with associated caves); however, the spatial occurrence has been poorly known. In order to evaluate the extent and distribution of karst development within the Castile portion of the Gypsum Plain, combined field and Geographic Information System (GIS) studies were conducted, which enable a first approximation of regional speleogenesis and delineate karst-related natural resources for management. Field studies included physical mapping of 50, 1-km^2 sites, including identification of karst features (sinkholes, caves, and springs) and geomorphic mapping. GIS-based studies involved analyses of karst features based on public data, including Digital Elevation Model (DEM), Digital Raster Graphic, (DRG) and Digital Orthophoto Quad (DOQ) formats. GIS analyses consistently underestimate the actual extent and density of karst development, based on karst features identified during field studies. However, DOQ analyses coupled with field studies appears to produce accurate models of karst development. As a result, a karst potential map of the Castile outcrop region was developed which reveals that karst development within the Castile Formation is highly clustered. Approximately 40% of the region effectively exhibits no karst development (<1 feature/km^2). Two small regions (<3 km^2 each) display intense karst development (>40 features/km^2) located within the northern extent of the Gypsum Plain, while many regions of significant karst development (>15 features/km^2) are distributed more widely. The clustered distribution of karst development suggests that speleogenesis within the Castile Formation is dominated by hypogenic, transverse processes.

INTRODUCTION

The gypsum facies of the Castile Formation crops out over an area of ~1800 km^2 in Eddy County, New Mexico and Culberson County, Texas on the western edge of the Delaware Basin (Fig. 1). The region has traditionally been referred to as the Gypsum Plain (Hill, 1996), which covers an area of ~2800 km^2 and is composed of outcrops of the Castile and Rustler Formations (Fig. 2). The region is located in the semi-arid southwest on the northern edge of the Chihuahuan Desert, where annual precipitation averages 26.7 cm with the greatest rainfall occurring as monsoonal storms in late summer (July – September) (Sares, 1984). Annual temperature averages 17.3 °C with an average annual minimum and maximum of 9.2 °C and 25.2 °C, respectively.

Throughout Castile outcrops, surficial karren occurs extensively in regions of exposed bedrock, including well-developed rillenkarren, spitzkarren, kamenitzas and tumuli. Sinkhole development is widespread, including both closed and open sinkholes ranging from near-circular features to laterally extensive, incised arroyo-like features. Cave development ranges widely, from small epigenic recharge features to large, complex polygenetic features (Stafford, 2006). The region hosts the second longest documented gypsum cave in North America, Parks Ranch Cave, Eddy County, N.M., with a surveyed length of 6596 m (Stafford, 2006). In addition, many other significant gypsum caves have been documented by the Texas Speleological Survey (TSS) (e.g., Reddell and Fieseler, 1977) and GYPsum KArst Project (GYPKAP) (Eaton, 1987; Belski, 1992; Lee, 1996). However, no systematic investigation has been conducted within the region with respect to karst development. Prior to this study, 246 karst features, primarily caves, were documented within the Castile outcrop region. The BLM (Bureau of Land Management) documented 45 of the total reported karst features (Jon Jasper, 2006, pers. com.); while the TSS

[1] Dept of Earth and Environmental Science, New Mexico Institute of Mining and Technology, Socorro, NM 87801, USA. kwstafford@juno.com, lagarde@nmt.edu and pboston@nmt.edu
[2] National Cave and Karst Research Institute, Carlsbad, NM, 88220, USA

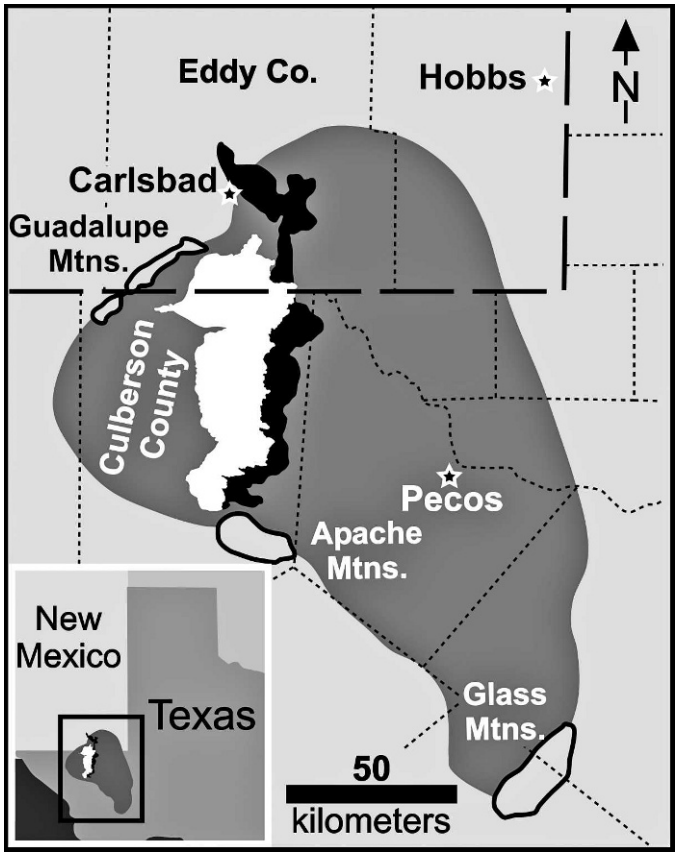

Figure 1. Location map showing location of Gypsum Plain including outcrop areas of the Castile Formation (solid white) and the Rustler Formation (solid black) within the Delaware Basin (dark gray), Eddy County, NM and Culberson County, Texas. Location of the Delaware Basin in relation to Texas and New Mexico is illustrated in bottom left corner, with the enlarged region outlined by the small black rectangle (adapted from Kelley, 1971, Dietrich et al., 1995 and Hill, 1996).

documented 201 of the total reported karst features (Jim Kennedy, 2006, pers. com.).

The rapid solution kinetics and high solubility of gypsum promotes extensive karst development. Gypsum solubility (2.53 g L^{-1}) is approximately three orders of magnitude greater than limestone (1.5 mg L^{-1}) in pure water and two orders of magnitude less than halite (360 g L^{-1}) (Klimchouk, 1996). The high solubility and near-linear solution kinetics of evaporites encourage intense surface dissolution that often forms large sinkholes, incised arroyos and caves that are laterally limited with rapid decreases in passage aperture away from inflows through epigenic speleogenesis (Klimchouk, 2000a). Additionally, the high solubilities of evaporites favor the development of hypogenic transverse speleogenesis driven by mixed convection (forced and free) (Klimchouk, 2000b). Forced convection is established by regional hydraulic gradients in confined settings, while free convection is generated where steep density gradients establish as fresh-waters are continuously supplied to the dissolution fronts (the upper levels) through the simultaneous sinking of saturated fluids by density differences (Anderson and Kirkland, 1980). Therefore epigenic and hypogenic karstic features likely both exist in the study area, often superimposed on each other.

The work we report here focuses on delineating the extent and distribution of karst development within the outcrop region of the Castile Formation, in order to predict regions of intense versus minimal karst development, which can be used for karst resource management as well as a first approximation for understanding regional speleogenesis. A dual approach involving field and Geographic Information System (GIS) analyses were utilized in order to define karst variability within the study area, including field mapping of 50, 1-km^2 regions and GIS analyses, using ESRI ArcGIS 9.2 software, of public data (i.e., Digital Elevation Model [DEM]; Digital Raster Graphic [DRG]; and Digital Orthophoto Quad [DOQ]) for the entire region. The combined results were used to develop a karst potential map of the Castile Formation outcrop region, while simultaneously evaluating different GIS-based techniques for karst analyses.

GEOLOGIC SETTING

The Castile Formation was deposited during the late Permian (early Ochoan), subsequent to deposition of the Guadalupian Capitan Reef, which is well-known for the caves it hosts in the Guadalupe Mountains (e.g., Hose and Pisarowicz, 2000). Castile evaporites represent deep-water deposits within a stratified, brine-filled basin (i.e., Delaware Basin) (Kendall and Harwood, 1989), bounded below by clastics of the Bell Canyon Formation, on the margins by Capitan Reef carbonates, and above by additional evaporitic rocks of the Salado and Rustler Formations (Fig. 2) (Kelley, 1971). Castile evaporites crop out along their western dissolution front in the Gypsum Plain (Fig. 1), dip to the east where they reach a maximum thickness of 480 m in the subsurface (Hill, 1996), and are characterized as massive to laminated sulfates (gypsum/anhydrite) interbedded with halite (Dietrich et al., 1995). Increased thickness in the east has been attributed to dissolution of intrastratal halite to the west and increased deposition to the east in the Ochoa Trough during the Permian (Anderson et al., 1972).

The Castile Formation, including outcrops in the Gypsum Plain, has experienced minimal tectonic deformation although located on the eastern edge of major tectonic events. Triassic and Laramide tectonism produced regional tilting to the northeast, broad flexures and fracturing with minimal offset within southeastern New Mexico and west Texas. The far western edge of the Delaware Basin has been down-dropped along the far eastern margin of Basin

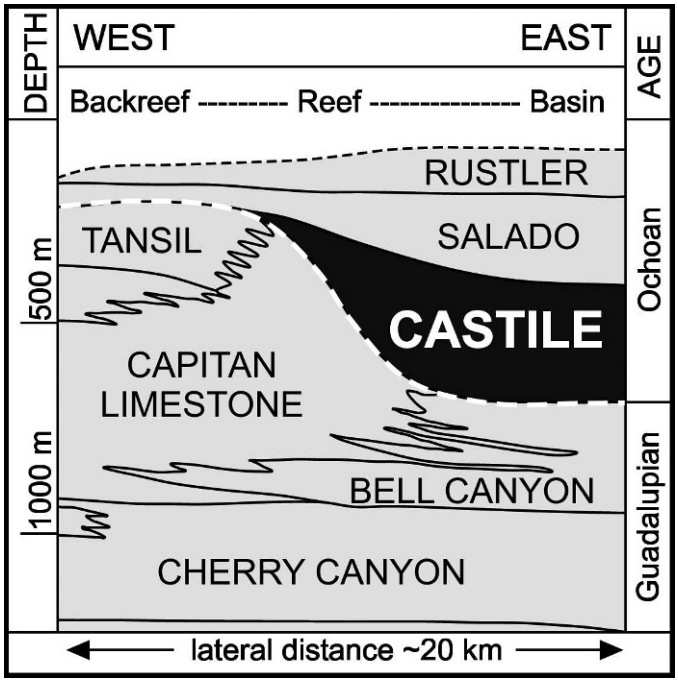

Figure 2. Diagrammatic representation of late Permian (Guadalupian and Ochoan) deposits associated with the Guadalupe Mountains (left) and Delaware Basin (right). Note that the Castile Formation fills in the basin and marks the beginning of the Ochoan (dashed white line) (adapted from Hill, 1996).

and Range block faulting; however, within the remaining Delaware Basin, the effects are limited to near-vertical joints (Horak, 1985). As a result of tectonism, Castile evaporites currently dip 3 to 5 degrees to the northeast with abundant conjugate joint sets oriented at ~ N75°E and ~N15°W. Associated with joint sets along the western dissolution front, solution subsidence valleys have developed from subsurface dissolution of halite beds (Hentz and Henry, 1989).

In addition to tectonic deformation, some sulfate rocks have been exposed to significant diagenesis. Original laminated (varved) gypsum often exhibits massive and nodular fabrics that are likely the result of plastic deformation associated with anhydrite/gypsum mineral conversion (Machel and Burton, 1991). Calcitized evaporites are common (often referred to as castiles or calcitized masses), generally forming clusters or linear trends of biogenic limestone associated with bacterial sulfate reduction (Kirkland and Evans, 1976). Selenite is locally abundant, forming linear features and fracture fillings (likely associated with mineral conversion), as well as lenticular masses (probably associated with calcitization processes). Diagenetic fabric alteration within Castile evaporites probably has exerted significant influence on establishing preferential flow paths for karst development within the Gypsum Plain.

Field Studies

Field mapping was conducted at 50, 1-km^2 sites within the Castile outcrop area (Fig. 3A). Field sites were randomly selected using ESRI ArcGIS 9.2 software in order to obtain an accurate representation of karst development within the Castile outcrop region and minimize any human biases that might be introduced into site selection. Ten field mapping sites were shifted up to two kilometers away from GIS-defined locations, in order to avoid anthropogenic features (i.e., roads, houses, quarries), while two sites were shifted up to four kilometers to avoid regions where land access was not available.

Each field site was defined as a one kilometer square region. Transect surveys were conducted on 100-meter line spacing, such that ten, one kilometer long transects were traversed in each of the 50 field sites. Smaller line-spacing (40 m) for transect surveys was compared with 100-meter line spacing through independent surveys by two of the authors at five field sites, which identified less than 10% additional karst features (i.e., sinkholes and caves). Because of the results of sub-sampling and the location of the study region within the semi-arid southwest, where vegetation is sparse and does not commonly obscure karst features, 100-meter spaced traverse surveys were found to be sufficient to document more than 90% of surficial karst features. During field mapping, identified feature locations were recorded with a hand-held GPS (Global Positioning System) and individual features were characterized based on size (length, width, depth), geomorphic expression (closed sink, open sink [i.e., cave], spring) and geologic occurrence (laminated, massive and nodular gypsum; gypsite; calcitized evaporite).

Field mapping identified 389 individual karst features, including 236 open sinkholes with free drains (i.e., caves or smaller solutional conduits that connect directly to sinkholes), 147 filled sinkholes, four caves with no associated sinkhole, and two springs. However, of the 236 open sinkholes, only 39 contained caves that were large enough to be humanly enterable. Of the 50 field sites, 12 contained no karst features and 14 sites contained more than 10 features (Fig. 4). Only two sites contained more than 30 features, one with 31 and one with 48.

Features were found in a wide range of gypsum fabrics (Fig. 5). Caves are largely developed in laminated (~43% of features) (Fig. 5A) and massive fabrics (~26% of features) (Fig. 5B); however, numerous small surficial caves form in gypsite (~28% of features) (Fig. 5D). Caves were occasionally found in selenite (<2% of features) (Fig. 5C) and calcitized masses (<2% of features) (Fig. 5E). Filled sinkholes were generally found in gypsite or alluvium; however, this likely only represents surficial mantling over deeper features in most cases.

Sinkhole area and volume ranged widely within the surveyed sites. The average open sinkhole area was 1.99×10^3 m^2 (0.3 to 4.12×10^4 m^2) with an average volume of

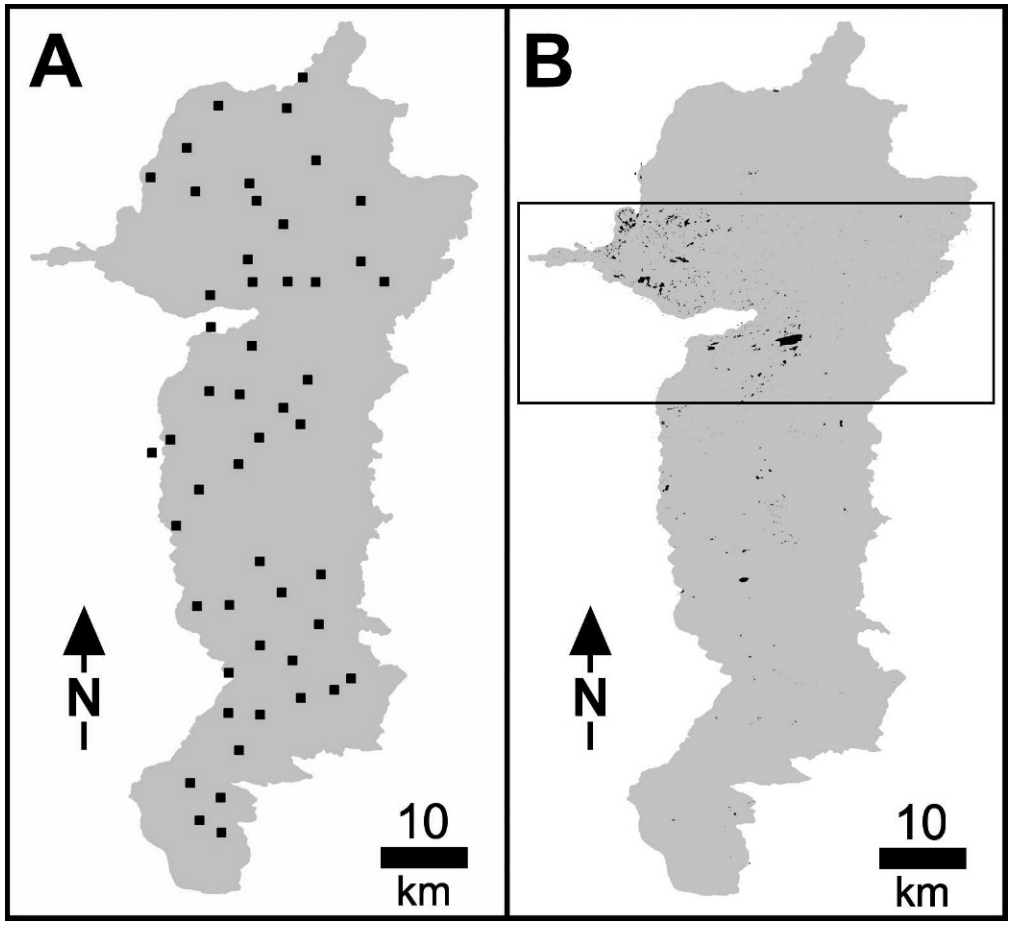

Figure 3. A) Castile outcrop region (gray) showing location of the 50 randomly selected 1 km^2 sites where field mapping was conducted; B) Castile outcrop region (gray) showing sinks (closed depressions) determined by DEM analysis (boxed area includes ~75% of the closed depressions identified through DEM analysis).

1.73×10^3 m^3 (8.0×10^{-2} to 4.71×10^4 m^3). The average area of closed sinkholes was 1.01×10^3 m^2 (3.0×10^{-2} to 2.36×10^4 m^2) with an average volume 3.70×10^2 m^3 (5.0×10^{-3} to 6.54×10^3 m^3). Sinkhole area was calculated by treating features as simple ellipses based on the maximum width and length measured in the field, while sinkhole volume was calculated by treating features as conical ellipses based on elliptical area and sinkhole depth. Therefore, approximated sinkhole areas and volumes probably overestimate true values.

GIS ANALYSES

In the last decade GIS has been recognized as a powerful tool for geographic analyses and has become a useful tool for cave and karst studies (e.g., Szukalski et al., 2002). Public data is available in multiple formats through government agencies, such as United States Geological Survey (USGS), New Mexico Bureau of Geology and Mineral Resources (NMBGMR), and Texas Natural Resource Inventory Service (TNRIS), which enables GIS analyses of large karst regions at zero cost.

GIS analyses of karst terrains have been used in various studies to delineate karst development. Florea et al. (2002) combined known point locations for karst features with digitized sinkholes from DRGs to develop karst potential maps in Kentucky, while Denizman (2003) conducted similar studies in Florida. Taylor et al. (2005) demonstrated the use of DEMs for delineating sinkholes in Kentucky. Hung et al. (2002) used an integrated approach involving analyses of multispectral imagery, aerial photography, and DEMs to evaluate relationships between lineaments and cave development.

Because most previous karst studies using GIS have focused on one or two techniques, multiple public data formats (DEM, DRG and DOQ) were compared and evaluated in this study, not only to characterize the extent of karst development but to also test the intercomparability of different methodologies. Physical mapping of karst features in the field, described in the previous section, was further compared with GIS techniques to fully evaluate the accuracy of GIS-based approaches. While field mapping identified the true occurrence of karst features within specific regions, the GIS analyses only represent approx-

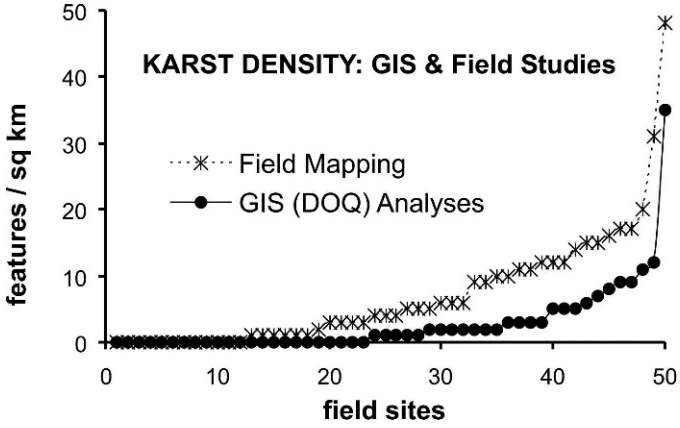

Figure 4. Comparative plot showing karst features identified during field mapping compared with features identified through DOQ analyses for the 50, 1 km^2 field sites. Field mapping and DOQ analyses are only shown because most DEM and DRG analyses showed no features in the regions where field mapping was conducted. Note that DOQ analysis identified ~35% of features that were located during field mapping.

imations based on the geomorphic expression of karst features (Fig. 6, 7).

Digital elevation models (DEM) were analyzed to define closed depressions (i.e., sinks) within the Castile outcrop region. Closed depressions were identified by creating a new DEM with filled sinks through GIS processing, which was compared with the original DEM to determine the difference between datasets (Fig. 3B, 6B) (Taylor et al., 2005). The resulting data included 554 individual sinkholes with an average area of 2.57×10^4 m^2 (6.0×10^2 to 8.70×10^5 m^2); however, approximately 80% of the identified features occurred within a 26 km (16 mile) wide strip immediately south of the New Mexico–Texas state line. Less than 5% of the features occurred north of the strip of abundant closed depressions, while the remainder was distributed south of the strip (Fig. 6B). Although all public data used for DEM analyses had 10-meter postings, the resulting sinkhole map suggests that there is significant variability in the source material used to create these DEMs. The region of sinkhole abundance appears to represent well the actual closed depressions within the study area, while regions outside this area appear to significantly underestimate feature abundance.

Digital raster graphics (DRG) of 1:24,000 USGS topographic maps were analyzed for the study area and all closed depressions were digitized as indicators of individual karst features (Fig. 6C, 7B); however, it is likely that multiple karst features exist within some large, closed depressions. From DRGs, 552 individual closed depressions were identified (Fig. 7B), with an average area of 1.54×10^4 m^2 (53 m^2 to 1.74×10^6 m^2), based on GIS spatial analyses. Because topographic maps of this region are based on 20 foot (6.1 m) contour intervals, numerous small sinkholes, including most of the features documented during field mapping, are not represented. However, most of the karst features documented by the BLM and TSS are represented as sinkholes on DRGs because topographic maps have traditionally been used for locating and identifying karst features.

Digital orthophoto quads (DOQ) within the study region have a resolution of one meter. DOQ analyses were conducted by visually picking probable karst features (Fig. 6D) at a resolution of 1:4,000. Features were identified based on geomorphic expression through comparison with known cave and karst features, either documented by the BLM in New Mexico and the TSS in Texas or features documented during field mapping. Based on comparison with known features, 3,237 individual features were identified within the Castile outcrop region (Fig. 7C).

Spatial analyses of feature densities were performed in order to delineate karst development within the study area. Three sets of data were processed separately to evaluate karst density, including: 1) known caves documented by the TSS and BLM (Fig. 7D); 2) DRG defined sinks (Fig. 7E); and 3) features identified through DOQ analyses (Fig. 7F). Density analyses of features identified from DEM data was not conducted because of the apparent high degree of variability in quality of these public data sets. All density analyses indicate intense karst development within the northwestern portion of the study area and a general decrease in feature abundance towards the east.

Discussion

Studies conducted to determine the extent and distribution of karst development vary widely (Veni, 2002), but GIS-based studies have enabled significant advances in geographic analyses within the last decade. Analyses of known karst distributions and features identified through GIS within the Castile outcrop region all show similar trends for areas of significant karst development. However, the degree of resolution of various public data used in GIS analyses produces substantial differences in evaluation of karst development throughout the entire region (Fig. 8), suggesting that field studies should always be coupled with any GIS-based studies. Sinkholes identified through DEM analyses were not used to develop karst density maps because of the apparent variability within the original data used to develop the DEMs. However, the DEM variability illustrates an important point, in that public data must be interpreted with caution.

Analysis of previously documented cave and karst features within the Castile outcrop region indicate small clusters of caves, focused in the northwestern region of the study area, largely along the dissolutional margin of the Castile Formation; however, only minor regions of karst development are observed scattered throughout the rest of

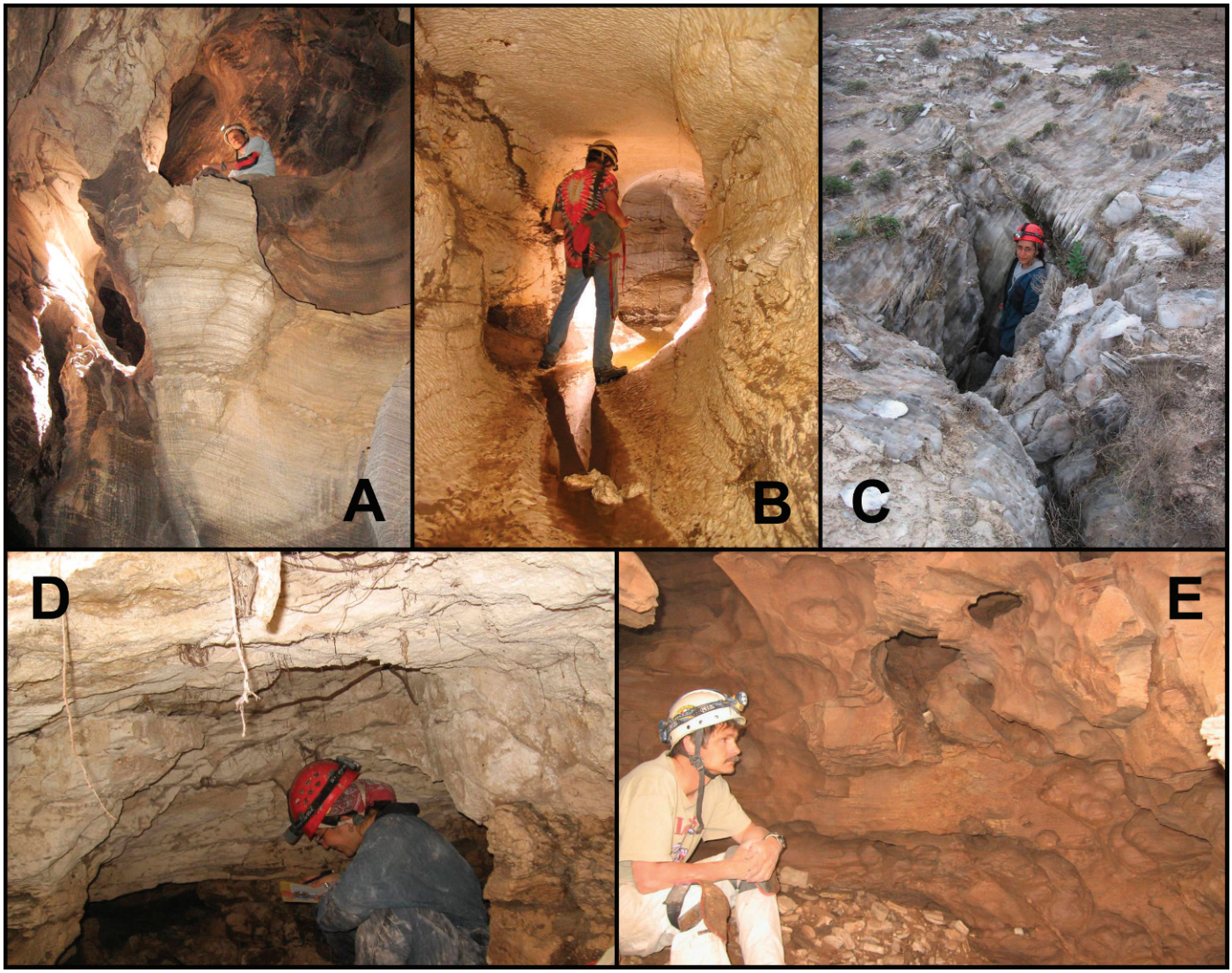

Figure 5. Cave development in the Castile Formation occurs within a wide range of lithologic fabrics. A) Plummet Cave: laminated gypsum; B) Parks Ranch Cave: massive gypsum; C) Black Widow Hole: selenite; D) Pokey Cave: gypsite, and e) Dead Bunny Hole: biogenic limestone (calcitized evaporite).

the study area (Fig. 7D). Based on previously documented features, approximately 95% of the study area effectively exhibits no karst development (<1 feature/km^2). Studies based on documented karst features inherently create biased results that may not accurately depict the complete distribution of karst development. Biases are introduced by variable access to portions of a karst region, such as regions where landowner access is not available or regions that are remote with poor road access.

Analysis of closed depressions depicted on DRGs (Fig. 7E) shows similar patterns of karst development as documented karst distributions (Fig. 7D), but do not show any regions with densities greater than 10 features/km^2. DRG analyses shows greater distributions of karst features than documented cave analyses, expanding the predicted boundaries of karst development; however, the majority of the study area (~90%) still appears to have minimal karst development (<1 feature/km^2). As with analyses of documented caves, DRGs appear to underestimate the actual extent of karst development because the contour interval of DRGs prevents distinguishable representation of small closed depressions and narrow, incised karst arroyos.

Analysis of karst features identified on DOQs indicates a significantly greater degree of karst development density and distribution (Fig. 7F) as opposed to other GIS-based analyses. Regions of minimal karst development were reduced to approximately 50% and several regions with karst feature densities greater than 15 features/km^2 were identified. Intense karst development still appears concentrated within the northwestern portion of the study area; however, regions of extensive karst development are

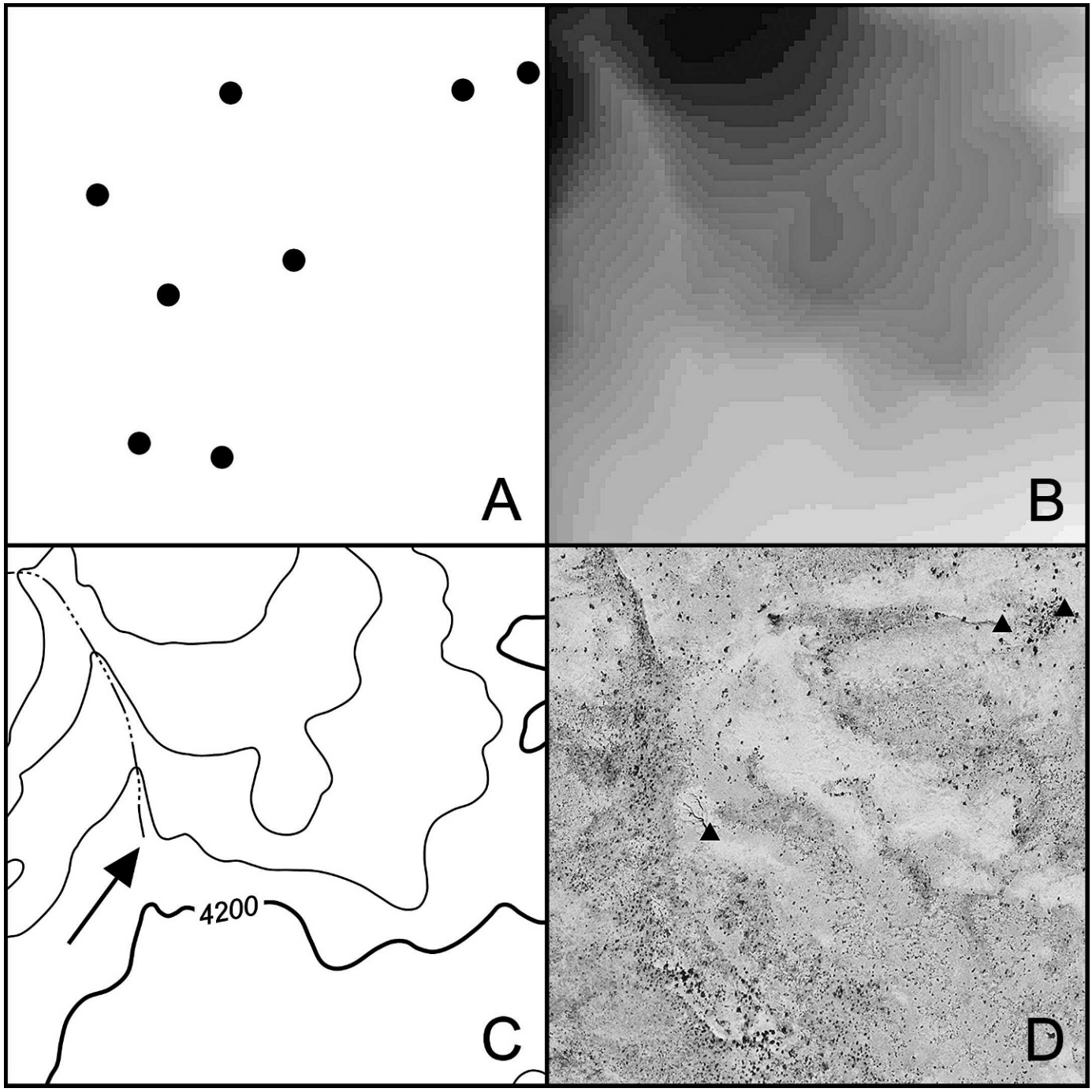

Figure 6. Variability in karst identification through various methodologies within a representative 1 km^2 field site (each square region measures 1 km by 1 km). A) filled black circles represent eight karst features documented through physical mapping of field site; B) original DEM of field site from which no karst features (closed depressions) were identified during GIS analysis (note darker shading in upper left is the highest elevations); C) DRG of field site showing no closed depressions, but a blind-terminated, ephemeral stream suggest sink point (arrow); and D) DOQ of field site showing geomorphic variability and the location of three features (black triangles) which could be resolved through DOQ analysis.

identified throughout the entire western half of the Castile outcrop area, as well as several smaller regions closer to the eastern margin of the study area. Although DOQ analysis shows more extensive karst development, it is inherently biased because features were visually picked based on comparison with the geomorphic expression of known features. Comparison of karst features physically documented during field studies with features identified through DOQ analysis, within the boundaries of field sites mapped, indicates that DOQ analysis consistently underestimates

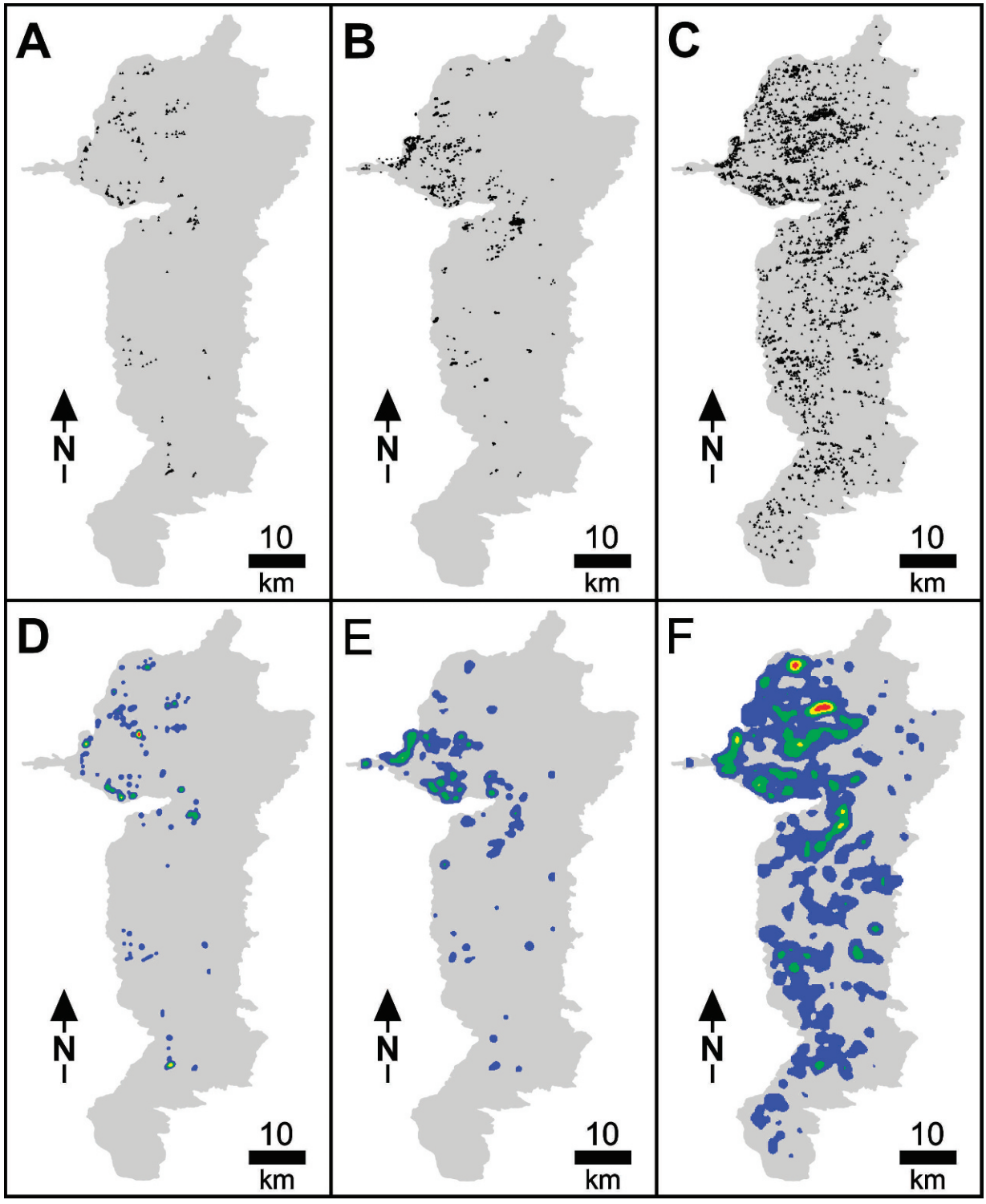

Figure 7. Comparison of data used for density analyses within the Castile outcrop region (grey). A) point data for individual karst features previously documented by the TSS and BLM; B) closed depressions digitized from DRGs; C) point data for individual karst features identified through DOQ analysis; D) karst feature density map based on previously documented karst features in Fig. 6A; E) karst feature density map based on distribution of individual closed depressions digitized from DRGs shown in Fig. 6B; and F) karst density map based on features identified through DOQ analysis shown in Fig. 6C. Color shading in karst density maps represent the number of karst features / km^2, where: gray $\leq$ 1 feature/km^2; blue = 1−5 features/km^2; green = 5−10 features/km^2; yellow = 10−15 features/km^2; and red $\geq$ 15 features/km^2.

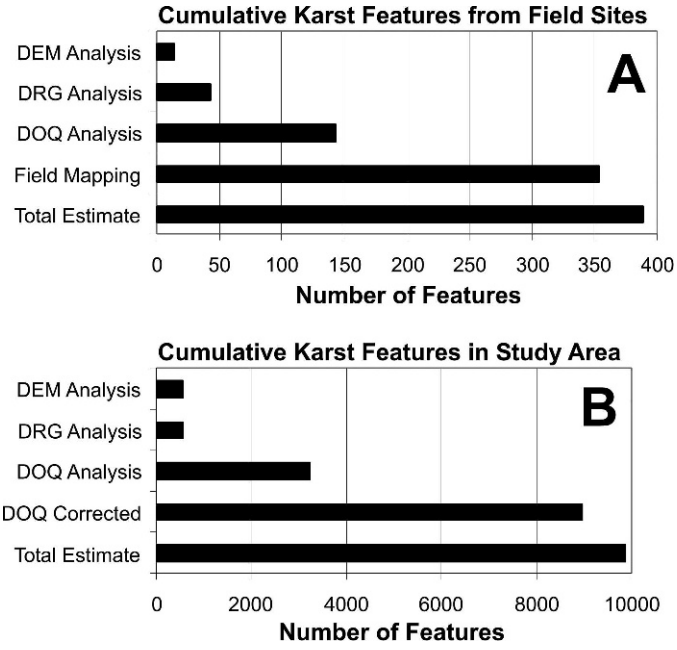

Figure 8. Comparative graphs of the results from various methodologies used to evaluate karst development within the Castile outcrop region. Note that Total Estimate refers to the 10% additional karst features expected based on field tests of smaller transect survey line spacing. A) Cumulative methodology results from the 50, 1-km^2 sites that were physically mapped during field studies. B) Cumulative karst features for the entire Castile outcrop region based on different methodologies, where DOQ Corrected represents the weighting DOQ-defined features by a factor of 2.77 based on the ratio of true features documented during field mapping with those identified through DOQ analysis.

the total number of karst features present (Fig. 4). This underestimation is likely the result of the 1-meter resolution of the DOQ public data.

DOQ analysis appears to best represent karst development within the outcrop region of the Castile Formation; however, all GIS-based analyses appear to under represent the extent of actual karst development as compared to physical karst surveys conducted in the field (Fig. 8). DOQ analyses generally identify 36% of the features documented during field studies (Figs. 4, 6, 7, and 8), while other GIS analyses commonly identify less than 5% of the features documented during field studies. Therefore, DOQ density analysis was weighted by a factor of 2.77 using Spatial Analyst, in order to adjust the densities calculated through GIS as compared to densities documented during field studies. As a result, a karst potential map was developed for the entire outcrop region of the Castile Formation (Fig. 9), which indicates that less than 40% of the outcrop region contains effectively no karst development (<1 feature/km^2), while two small regions (<3 km^2 each) within New Mexico exhibit intense karst development (>40 features/km^2). Comparative tests of line spacing used in transect-based field mapping, suggests that the actual density of karst features may be at least 10% greater (Fig. 8). The karst potential map likely represents karst development relatively accurately within the study area, but a complete physical survey of the entire 1,800 km^2 region would probably show discrepancies.

Conclusions

The development of a karst potential map for the Castile Formation shows that karst development is distinctly clustered within the Gypsum Plain (Fig. 9). Visual interpretation of the clustering distribution of karst features within the Castile outcrop region was confirmed through GIS-based nearest neighbor analyses (Ford and Williams, 1989), which yielded a nearest neighbor index of 0.439. A nearest neighbor index of 1 is classified as random while values greater than 1 approach a regular, evenly spaced pattern while values less than 1 approach greater clustering (Ford and Williams, 1989). A nearest neighbor index of 0.439 indicates significant clustering. Large regions exhibit minimal surficial karst expressions, primarily along the southern and eastern edges of the Castile outcrop area.

The densest regions occur in the northwestern portion of the outcrop area, and commonly contain more than 20 features/km^2 (Fig. 9), with more than 40 features/km^2 locally. The northern of the two densest regions contains the second longest known gypsum cave in North America, Parks Ranch Cave, and is largely included within a BLM critical resource area that does not allow surface occupancy, thus protecting the extensive karst development within this area. However, the second dense karst region should be evaluated through more intense field studies to determine if it should also be protected as a critical resource area.

GIS-based analyses have become an important tool for karst studies. DOQ analysis, coupled with field studies, has been shown to be the most effective method for delineating the actual extent and intensity of karst development within the Castile outcrop area, because of the sparse vegetation associated with the semi-arid southwestern United States. However, this may not be the most effective technique in other regions where vegetation is denser. Although commonly used in many karst regions, DRG analysis within the study area proved to poorly represent the actual extent of karst development within the region because of the low resolution of contour intervals, including significantly underestimating the actual abundance of karst features within the two densest regions. DEM analysis proved to be of little use within the study area, because apparent variability in original data from which the DEMs were constructed does not consistently represent the same resolution.

Although DEM and DRG analyses proved ineffective in the study area, it is likely that these methodologies could

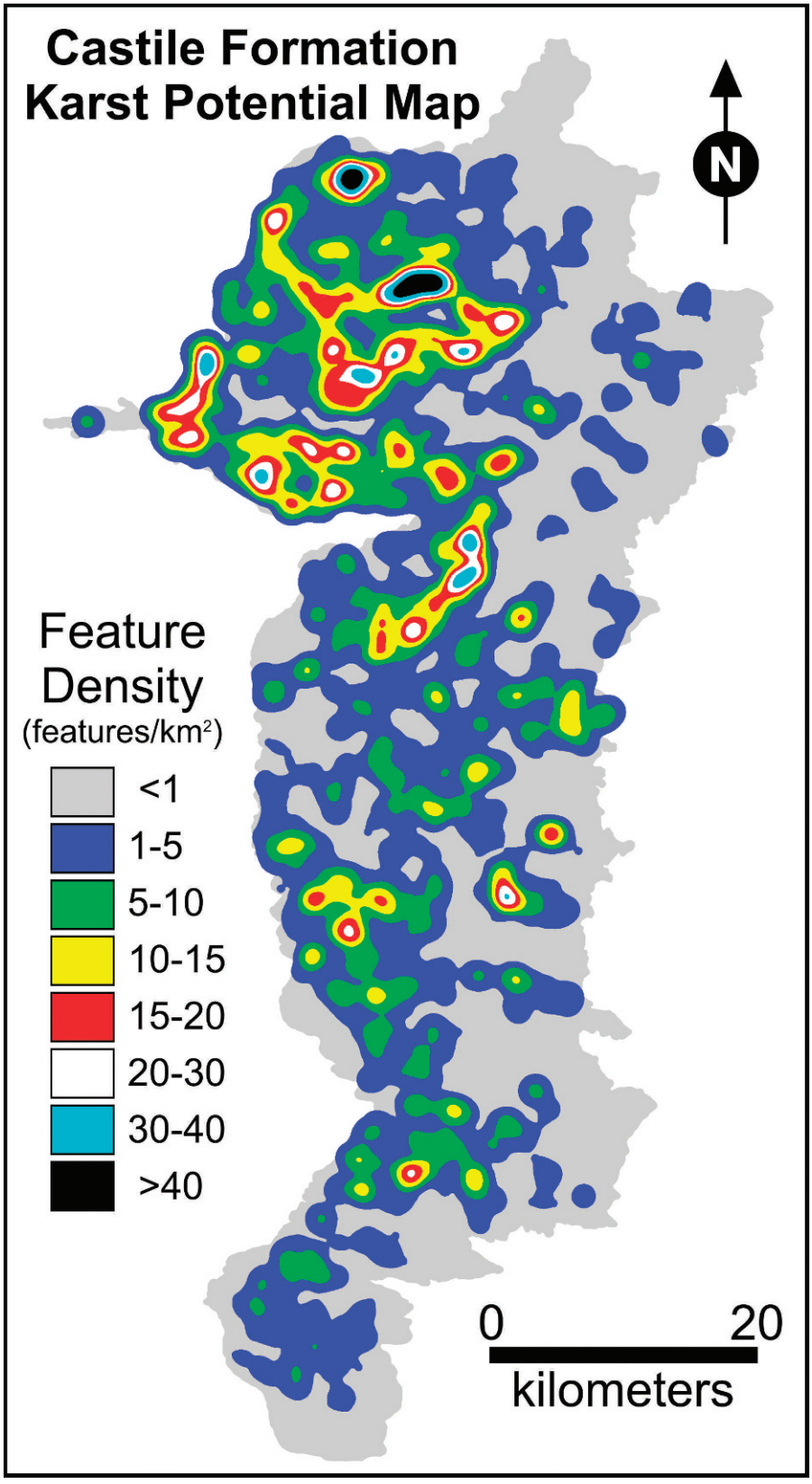

Figure 9. Karst potential map of the Castile Formation outcrop region defined in this study. Note the two dense areas of karst development within the northern portion of the study area with densities greater than 40 features/km^2.

be effective for delineating karst development in other regions where higher resolution DEM or DRG data is available. Ultimately, the scale of karst features within regions being evaluated with GIS methodologies must be compared with the resolution of available GIS data, in order to determine the effectiveness of GIS-based studies. Therefore, caution must be taken when conducting GIS-based karst analyses, which should always be coupled with field studies for verification, not only in densely karsted areas, but also in regions that appear to have minimal karst development.

The distinct clustering pattern of karst provides some insight into the nature of speleogenesis within the region (Figs. 7, 9). Klimchouk (2003) and Frumkin and Fischhendler (2005) suggest that hypogenic karst tends to form in dense clusters separated by regions of minimal karst development because heterogeneities within soluble strata promote transverse speleogenesis in regions where rising fluids become focused along favorable flow paths. In contrast, epigenic karst is generally expressed as more widely distributed features where descending meteoric waters attempt to utilize all available irregularities near the surface and converge with depth. Because convergence occurs with depth in epigenic karst, surficial expressions tend to be less clustered in epigenic dominated karst as opposed to hypogenic karst where convergence occurs near the surface.

Current studies of karst development within the Castile Formation by the authors have found significant morphological evidence within individual caves that supports the interpretation of speleogenesis dominated by hypogene processes. These include the diagnostic suite of hypogenic features (e.g. risers, channels and cupolas) reported by Klimchouk (2007), as well as the widespread occurrence of blanket breccias (Anderson et al., 1978), breccia pipes (Anderson and Kirkland, 1980), evaporite calcitization (Kirkland and Evans, 1976) and native sulfur deposits (Hentz and Henry, 1989) previously reported within the region. Current research is focusing on interpreting the speleogenetic evolution of the Castile Formation, including the diagenetic alteration of calcium sulfate rocks and the development of cavernous porosity. However, this is beyond the scope of this manuscript and will be reported separately in the near-future. While GIS-based analyses provide insight into the speleogenetic processes of the region, detailed field studies of specific features will be required in order to interpret the speleogenetic evolution of the region.

While the karst potential map of the Castile Formation outcrop region alone can only provide limited insight into regional speleogenesis, it can provide an effective tool for land management within Eddy County, New Mexico and Culberson County, Texas. Delineation of karst intense regions can be used in land management planning for road construction and oilfield well and pipeline placements, in order to not only avoid regions of potential geohazards associated with collapse, but also to protect regions of significant ground-water recharge. Whether Castile karst is primarily the result of hypogenic or epigenic speleogenesis, most exposed features currently act as ground-water recharge features, thus the delineation of dense karst regions is crucial for the sustained management of sparse water resources within this portion of the semi-arid southwest. Ultimately, karst potential maps can be used to delineate sensitive regions for karst resource management.

Acknowledgements

The authors are indebted to Jack Blake, Draper Brantley, Stanley Jobe, Lane Sumner and Clay Taylor for their generous access to private ranches in Texas throughout this study. Tim Hunt provided useful information and assistance with University Land in Texas. Jon Jasper and Jim Goodbar provided essential information about known gypsum karst development within New Mexico. Jim Kennedy provided essential information about known gypsum karst development within Texas. The authors are thankful for the useful comments provided by an anonymous reviewer and Amos Frumkin which helped to improve this manuscript. This research was partially funded through grants from the New Mexico Geological Society and the New Mexico Tech Graduate Student Association and support from the National Cave and Karst Research Institute (NCKRI).

References

Anderson, R.Y., Dean, W.E., Kirkland, D.W., and Snider, H.I., 1972, Permian Castile varved evaporite sequence, West Texas and New Mexico: Geological Society of America Bulletin, v. 83, p. 59–85.

Anderson, R.Y., Kietzke, K.K., and Rhodes, D.J., 1978, Development of dissolution breccias, northern Delaware Basin and adjacent areas: New Mexico Bureau of Mines and Mineral Resources Bulletin 159, p. 47–52.

Anderson, R.Y., and Kirkland, D.W., 1980, Dissolution of salt deposits by brine density flow: Geology, v. 8, p. 66–69.

Belski, D., ed., 1992, GYPKAP Report Volume #2: Southwestern Region of the National Speleological Society, Albuquerque, N.M., 57 p.

Denizman, C., 2003, Morphometric and spatial distribution parameters of karstic depressions, lower Suwannee River basin, Florida: Journal of Cave and Karst Studies, v. 65, no. 1, p. 29–35.

Dietrich, J.W., Owen, D.E., Shelby, C.A., and Barnes, V.E., 1995, Geologic atlas of Texas: Van Horn-El Paso Sheet: University of Texas Bureau of Economic Geology, Austin, Texas,

Eaton, J., ed., 1987, GYPKAP 1987 Annual Report: Southwestern Region of the National Speleological Society, Alamogordo, N.M., 35 p.

Florea, L.J., Paylor, R.L., Simpson, L., and Gulley, J., 2002, Karst GIS advances in Kentucky: Journal of Cave and Karst Studies, v. 64, no. 1, p. 58–62.

Ford, D.C., and Williams, P.W., 1989, Karst Geomorphology and Hydrology: London, Unwin Hymam, 601 p.

Frumkin, A., and Fischhendler, I., 2005, Morphometry and distribution of isolated caves as a guide for phreatic and confined paleohydrological conditions: Geomorphology, v. 67, p. 457–471.

Hentz, T.F., and Henry, C.D., 1989, Evaporite-hosted native sulfur in Trans-Pecos Texas: Relation to late-phase Basin and Range deformation: Geology, v. 17, p. 400–403.

Hill, C.A., 1996, Geology of the Delaware Basin, Guadalupe, Apache and Glass Mountains: New Mexico and West Texas: Permian Basin Section: Midland, Texas, SEPM, 480 p.

Horak, R.L., 1985, Trans-Pecos tectonism and its affects on the Permian Basin, *in* Dickerson, P.W., and Muelberger, W.R., eds., Structure and Tectonics of Trans-Pecos Texas: Midland, Texas, West Texas Geological Society, p. 81–87.

Hose, L.D., and Pisarowicz, J.A., eds., 2000, The Caves of the Guadalupe Mountains: Journal of Cave and Karst Studies, v. 62, no. 2, 157 p.

Hung, L.Q., Dinh, N.Q., Batelaan, O., Tam, V.T., and Lagrou, D., 2002, Remote sensing and GIS-based analysis of cave development in the Suoimuoi Catchment (Son La – NW Vietnam): Journal of Cave and Karst Studies, v. 64, no. 1, p. 23–33.

Kelley, V.C., 1971, Geology of the Pecos Country, Southeastern New Mexico: New Mexico Bureau of Mines and Mineral Resources, 78 p.

Kendall, A.C., and Harwood, G.M., 1989, Shallow-water gypsum in the Castile Formation – significance and implications, *in* Harris, P.M., and Grover, G.A., eds., Subsurface and Outcrop Examination of the Capitan Shelf Margin, Northern Delaware Basin: SEPM, Core Workshop No. 13, San Antonio, Texas, p. 451–457.

Kirkland, D.W., and Evans, R., 1976, Origin of limestone buttes, Gypsum Plain, Culberson County, Texas: American Association of Petroleum Geologists Bulletin, v. 60, p. 2005–2018.

Klimchouk, A., 1996, Dissolution and conversion of gypsum and anhydrite: International Journal of Speleology, v. 25, no. 3–4, p. 263–274.

Klimchouk, A., 2000a, Speleogenesis in gypsum, *in* Klimchouk, A., Ford, D.C., Palmer, A.N., and Dreybrodt, W., eds., Speleogenesis: Evolution of Karst Aquifers: Huntsville, National Speleological Society, Inc., p. 261–273.

Klimchouk, A., 2000b, Speleogenesis under deep-seated and confined conditions, *in* Klimchouk, A., Ford, D.C., Palmer, A.N., and Dreybrodt, W., eds., Speleogenesis: Evolution of Karst Aquifers: Huntsville, National Speleological Society, Inc., p. 244–260.

Klimchouk, A., 2003, Conceptualization of speleogenesis in multi-story artesian systems: a model of transverse speleogenesis: Speleogenesis and Evolution of Karst Aquifers, v. 1, no. 2, p. 1–18.

Klimchouk, A., 2007, Hypogene Speleogenesis: Hydrogeological and Morphometric Perspective: Carlsbad, National Cave and Karst Research Institute, Special Paper No. 1, 106 p.

Lee, J., ed., 1996, GYPKAP Report Volume 3: Southwestern Region of the National Speleological Society, 69 p.

Machel, H.G., and Burton, E.A., 1991, Burial-diagenetic sabkha-like gypsum and anhydrite nodules: Journal of Sedimentary Petrology, v. 61, no. 3, p. 394–405.

Reddell, J.R., and Fieseler, R.G., 1977, The Caves of Far West Texas: Austin, Texas Speleological Survey, 103 p.

Sares, S.W., 1984, Hydrologic and geomorphic development of a low relief evaporite karst drainage basin, southeastern New Mexico [M.S. Thesis]: Albuquerque, University of New Mexico, 123 p.

Stafford, K.W., 2006, Gypsum karst of the Chosa Draw area, *in* Land, L., Lueth, V.W., Raatz, W., Boston, P., and Love, D., eds., Caves and Karst of Southeastern New Mexico: Socorro, New Mexico Geological Society Fifty-seventh Annual Field Conference, New Mexico Geological Society, p. 82–83.

Szukalski, B.W., Hose, L.D., and Pisarowicz, J.A., eds., 2002, Cave and karst GIS: Journal of Cave and Karst Studies, v. 64, no. 1, 93 p.

Taylor, C.J., Nelson, H.L., Hileman, G., and Kaiser, W.P., 2005, Hydrogeologic-framework mapping of shallow, conduit-dominated karst — components of a regional GIS-based approach, *in* U.S. Geological Survey Karst Interest Group Proceedings, Rapid City, South Dakota, U.S. Geological Survey Scientific Investigations Report 2005–5160, p. 103–113.

Veni, G., 2002, Revising the karst map of the United States: Journal of Cave and Karst Studies, v. 64, no. 1, p. 45–50.